Macromolecules

ARTICLE

pubs.acs.org/Macromolecules

Morphological Transition from Spherical to Lamellar Nanophases in Epoxy Thermosets Containing Poly(ethylene oxide)-*block*-poly(ε-caprolactone)-*block*-polystyrene Triblock Copolymer by Hardeners

Rentong Yu and Sixun Zheng*

Department of Polymer Science and Engineering and State Key Laboratory of Metal Matrix Composites, Shanghai Jiao Tong University, Shanghai 200240, P. R. China

ABSTRACT: In this study, we synthesized poly(ethylene oxide)-*block*-poly(ε-caprolactone)-*block*-polystyrene (PEO-*b*-PCL-*b*-PS) triblock copolymer via the combination of ring-opening polymerization (ROP) and atomic transfer radical polymerization (ATRP). The ABC triblock copolymer was incorporated into epoxy to access the nanostructured thermosets. It is found that the nanophases of the epoxy thermosets can be modulated by using different hardeners. While cured with 4,4′-methylenebis(2-chloroaniline), the thermosets displayed the long-ranged ordered nanostructures in which the spherical nanophases were arranged into body-centered cubic (*bcc*) lattice at the compositions investigated. While 4,4′-diaminodiphenylsulfone was used as the hardener, the thermosets displayed the lamellar nanostructure. The formation of nanostructures in the thermosets has been evidenced by atomic force microscopy and small-angle X-ray scattering. The morphological transition from spherical to lamellar nanophases has been interpreted in terms of the microphase separation of different subchains of the ABC triblock copolymer out of the epoxy−amine matrix during the curing reactions owing to the dependence of miscibility of epoxy networks with PCL subchain of the triblock copolymer on types of hardeners. The kinetics of curing and microphase separation shows the tandem reaction-induced microphase separation occurred while DDS was used as the hardener, which gave rise to the formation of lamellar nanostructures in the epoxy thermosets containing the ABC triblock copolymer.

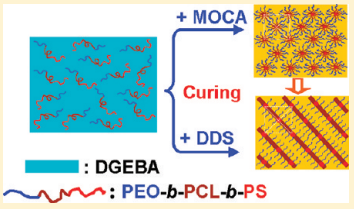

INTRODUCTION

The concept of incorporating block copolymers into thermosets has been accepted to be one of the most efficient approaches to access ordered or disordered nanostructures in thermosets since Hillmyer et al. first reported the creation of nanostructures in epoxy thermosets with an amphiphilic block copolymers in 1997.[1,2] The formation of nanostructures can greatly optimize the intercomponent interactions between thermosetting matrix and modifiers and thus the mechanical properties of thermosets can be further improved.[3,4] More recently, it has been explored to utilize the nanostructured thermosets as the precursors of other nanomaterials with some new and functional properties.[5,6] The formation of nanostructures in thermosets by the use of block copolymers can follow two different mechanisms: (i) self-assembly[1,2] and (ii) reaction-induced microphase separation.[7,8] Hillmyer et al.[1,2] first reported the strategy of creating nanostructures via self-assembly approach. In the protocol, the precursors of thermosets act as the selective solvents of block copolymers and various ordered or disordered nanostructures are formed in the mixtures depending on the blend composition before curing reaction. These nanophases can be further fixed via subsequent curing with introduction of hardeners although there are some minor changes in morphology with the occurrence of the curing reactions. The self-assembly approach is based on the equilibrium thermodynamics in the mixtures of precursors of thermosets with amphiphilic block copolymers and thus can be taken as a templating technique due to the presence of preformed nanophases.[1,2] More recently, Zheng et al.[7,8] reported that ordered or disordered nanostructures in thermosets can be alternatively formed via so-called reaction-induced microphase separation mechanism (RIMPS). In this approach, it is not required that the amphiphilic block copolymers are self-organized into nanophases prior to curing reaction; i.e., all the subchains of block copolymers can be miscible with precursors of thermosets. With the occurrence of curing reaction, a part of subchains of block copolymers are microphase-separated out whereas other blocks still remain mixed with thermosets. In marked contrast to self-assembly approach, RIMPS can be additionally affected by the competitive kinetics of curing reaction and microphase separation and this can provide ones with tremendous space for maneuver to modulate the nanostructures in thermosets by adjusting some thermodynamic and kinetic factors such as competitive kinetics (or dynamics) between microphase separation and polymerization. During the past few years, the self-assembly approach has been extensively investigated vis-à-vis RIMPS behavior in thermosets.[1,2,5−38]

In previous studies, considerable efforts have been made to investigate the formation of nanostructures via self-assembly or RIMPS approach by using a variety of block copolymer architectures.[1,2,5−39] However, the effect of the natures of cross-linked networks on formation of nanostructures was less investigated.[17] Rebizant et al.[17] examined the effect of hardeners

Received: June 26, 2011
Revised: September 14, 2011
Published: October 04, 2011

ACS Publications © 2011 American Chemical Society

on the nanostructures in epoxy thermosets containing polystyrene-*block*-polybutadiene-*block*-poly(methyl methacrylate-*stat*-methyl acrylate) triblock copolymer and found that spherical nanophases were formed while the thermosets were cured with 4,4′-methylenebis(3-chloro-2,6-diethylaniline) (MCDEA), 4,4′-methylenedianiline (MDA) and 2-phenylimidazole (2-PI) [alone or with methyltetrahydrophthalic anhydride (MTHPA) as comonomer], respectively. While the thermosets were cured with 4,4′-diaminodiphenyl sulfone or dicyandiamide/*N*,*N*″-(4-methyl-1,3-phenylene)bis(*N*′,*N*′-dimethylurea), macroscopic aggregates or vesicles were formed in the thermosets. It is proposed that the effect of cross-linked networks is by no means trivial since the thermodynamics and kinetics involving the formation of nanostructures in thermosets are significantly dependent on the natures of the cross-linked networks. However, such an investigation remains largely unexplored.

In this work, we present an investigation on the formation of nanostructures in epoxy thermosets containing poly(ethylene oxide)-*block*-poly(ε-caprolactone)-*block*-polystyrene ABC triblock copolymer (PEO-*b*-PCL-*b*-PS). The purpose of this work is to investigate the effect of cross-linked networks on the formation of nanostructures in the thermosets by using different hardeners. The utilization of the PEO-*b*-PCL-*b*-PS terpolymer is based on the following knowledge: (i) PEO is miscible with epoxy[39−42] whereas reaction-induced phase separation always occurs in the blends of epoxy with PS[8,31,44,45] and (ii) the phase behavior of epoxy-PCL blends is quite dependent on type of hardeners.[46−48] It has been reported that with dianhydrides as the hardeners reaction-induced phase separation can take place in the blends of epoxy with PCL.[46] In contrast, the thermosetting blends are generally miscible while diamines were used as the hardeners. The miscibility of diamine-cross-linked blends has been attributed to the formation of the intermolecular specific interactions (viz. hydrogen bonding) in the thermosetting blends.[47] Nonetheless, Chang[48] reported the immiscibility in the blends of epoxy with PCL while 4,4′-diaminodiphenylsulfone, an aromatic amine was used as the hardener. It was identified that the reaction-induced phase separation can follow either spinodal decomposition or nucleation and growth mechanism depending on PCL concentration in the blends. The different phase behavior in the blends with different diamine hardeners has been interpreted according to the difference in the intermolecular specific interactions (viz. hydrogen bonding).[49] The dependence of the miscibility of epoxy-PCL blends on hardeners could provide ones with a possibility to modulate nanostructures in epoxy thermosets containing PEO-*b*-PCL-*b*-PS triblock copolymer by using different hardeners.

In this study, both 4,4′-methylenebis(2-chloroaniline) (MOCA) and 4,4′-diaminodiphenylsulfone (DDS) were respectively used as the hardeners to control over the formation of nanostructures in the thermosets. It has been known that MOCA-cured blends of epoxy with PCL are fully miscible whereas those cured with DDS are phase-separated.[43,49,50] Therefore, it is anticipated that the nanostructures in epoxy thermosets containing PEO-*b*-PCL-*b*-PS terpolymer can be modulated by the use of the above two hardeners. In this work, the nanostructures of thermosets were investigated by means of atomic force microscopy (AFM), small-angle X-ray scattering (SAXS) and dynamic mechanical thermal analysis (DMTA). The formation of nanostructures was addressed on the basis of tandem reaction-induced microphase separation while DDS was used as the hardener.

EXPERIMENTAL SECTION

Materials. Diglycidyl ether of bisphenol A (DGEBA) with epoxide equivalent weight of 185−210 was purchased from Shanghai Resin Co., China. Both 4,4′-methylenebis(2-chloroaniline) (MOCA) and 4,4′-diaminodiphenylsulfone (DDS) were used as the hardeners, purchased from Shanghai Reagent Co., China. Poly(ethylene oxide) monomethyl ether (MPEO5000) with a molecular weight of M_n = 5000 and ε-caprolactone (99%) (ε-CL) were purchased from Fluka Co., Germany. Before use, ε-CL was distilled over calcium hydride (CaH_2) under decreased pressure. Stannous octanoate [$Sn(Oct)_2$] was purchased from Aldrich Co. USA. Styrene (St) was purchased from Shanghai Reagent Co., China. Prior to use, the inhibitor was removed by washing with aqueous sodium hydroxide (5 wt %) and deionized water for at least three times and then dried by anhydrous magnesium sulfate; the monomers were further distilled under reduced pressure. 2-Bromoisobutyryl bromide and *N*,*N*,*N*′,*N*′,*N*″-pentamethyldiethylenetriamine (PMDETA) were purchased from Aldrich Co. USA and used as received. Triethylamine was dried over CaH_2 and then was refluxed with *p*-toluenesulfonyl chloride, followed by distillation. Copper(I) bromide (CuBr) was obtained from Shanghai Reagent Co., China. All other reagents and solvents used in this work were purchased from Shanghai Reagent Co., China. Before use, toluene and tetrahydrofuran were refluxed over sodium and then distilled.

Synthesis of PEO-*b*-PCL Diblock Copolymer. The PEO-*b*-PCL diblock copolymer was synthesized via ring-opening polymerization of ε-caprolactone (ε-CL) with monohydroxyl-terminated PEO as the macromolecular initiator and $Sn(Oct)_2$ as the catalyst. Typically, monohydroxyl-terminated PEO (12.8505 g, 2.57 mmol) and ε-CL (21.4 g, 187.5 mmol) were charged to a 100 mL round-bottom flask equipped with a dried magnetic stirring bar; $Sn(Oct)_2$ [at a ratio of 1.6/1000 (w/w) with respect to ε-CL] was added with a syringe. The reactive mixture was connected to a standard Schlenk line to degas via three pump−freeze−thaw cycles. The polymerization was carried out at 120 °C for 38 h to access the complete conversion of ε-CL. The crude product was dissolved in tetrahydrofuran and the solution was dropwise added into a great amount of petroleum ether to afford the precipitates. This procedure was repeated thrice to purify the sample. The product was dried at 30 °C in vacuum oven for 48 h and 33.7326 g product was obtained with the yield of 98%. The molecular weight of the diblock copolymer was measured by means of gel permeation chromatography to be M_n = 13 160 with M_w/M_n = 1.10.

Synthesis of PEO-*b*-PCL-*b*-PS Triblock Copolymer. The above PEO-*b*-PCL diblock copolymer was used to react with 2-bromoisobutyryl bromide in the presence of triethylamine to afford a 2-bromoisobutyryl-terminated PEO-*b*-PCL diblock copolymer [denoted PEO-*b*-PCL−$OOCC(CH_3)_2Br$], which was further used as the macromolecular initiator for atom transfer radical polymerization of styrene to obtain PEO-*b*-PCL-*b*-PS triblock copolymer. Typically, the above PEO-*b*-PCL−$OOCC(CH_3)_2Br$ macromolecular initiator (4.8004 g, 0.36 mmol), CuBr (0.0519 g, 0.36 mmol), PMDETA (72 μL, 0.36 mmol), and styrene (7.1914 g, 69 mmol) were charged to a flask. The flask was connected to a standard Schlenk line system to degas via three pump−freeze−thaw cycles. The polymerization was carried out at 110 °C for 5 h and then the system was cooled to room temperature. The solvent THF was added to dissolve the reacted mixture. The mixture was passed over a column of neutral alumina to remove the catalyst. The solution was concentrated and then dropped into a great amount of petroleum ether to afford the precipitates. This procedure was repeated thrice to purify the sample. The precipitates were dried *in vacuo* at 30 °C for 48 h and 7.6632 g of product was obtained with the conversion of styrene monomer to be *ca.* 40%. The molecular weight of PEO-*b*-PCL-*b*-PS was measured by means of gel permeation chromatography to be M_n = 21 000 with M_w/M_n = 1.06.

Synthesis of Model PCL and PS. The model poly(ε-caprolactone) (PCL) was synthesized via ring-opening polymerization (ROP) of ε-CL with benzyl alcohol as the initiator and $Sn(Oct)_2$ was used as the catalyst. Typically, benzyl alcohol (0.0704 g, 0.65 mmol) and ε-CL (5.5950 g, 49 mmol) were charged to a 50 mL round-bottom flask equipped with a dried magnetic stirring bar, and $Sn(Oct)_2$ (1/1000 wt with respect to ε-CL) was added with a syringe. The flask was connected to a standard Schlenk line, and the reactive mixture was degassed via three freeze−pump−thaw cycles and then immersed in a thermostated oil bath at 120 °C for 36 h. The crude product was dissolved in tetrahydrofuran, and the solution was dropped into an excess amount of petroleum ether to afford the precipitates. This procedure was repeated three times to obtain white the solids with the yield of 98%. The molecular weight of the PCL was estimated to be M_n = 8400 according to the ratio of integration intensity of aliphatic methylene protons to aromatic protons in its ^1H NMR spectrum.

The PS homopolymer with the molecular weight comparable to the length of PS in the PEO-*b*-PCL-*b*-PS triblock copolymer was synthesized via atom transfer radical polymerization (ATRP), and methyl 2-bromopropionate was used as the initiator. Styrene (10.2400 g, 98.3 mmol), Cu^IBr (0.0923 g, 0.64 mmol), and PMDETA (133 μL, 0.64 mmol) were charged to a 50 mL flask equipped with a magnetic stirrer, and methyl 2-bromopropionate (0.1083 g, 0.64 mmol) was added with a syringe. The system was connected to the Schlenk line system, and three freeze−pump−thaw cycles were used to remove the trace of moisture and oxygen. The polymerization was carried out at 110 °C for 2 h and the conversion of styrene was controlled within 52% and the molecular weight was determined to be M_n = 8200 with M_w/M_n =1.10 as measured by means of GPC.

Preparation of Epoxy Thermosets Containing PEO-*b*-PCL-*b*-PS. Desired amount of the PEO-*b*-PCL-*b*-PS was dissolved in DGEBA, and then stoichiometric MOCA (and/or DDS) with respect to DGEBA was added with continuous stirring until the mixtures were totally homogeneous. The ternary mixtures were poured into Teflon molds and cured at 150 °C for 4 h plus 180 °C for 2 h.

MEASUREMENT AND CHARACTERIZATION

Nuclear Magnetic Resonance Spectroscopy (NMR). The samples were dissolved in deuterium chloroform, and the NMR spectra were measured on a Varian Mercury Plus 400 MHz NMR spectrometer with tetramethylsilane (TMS) as the internal reference.

Gel Permeation Chromatography (GPC). The molecular weights and molecular weight distribution of polymers were determined on a Waters 717 Plus autosampler gel permeation chromatography apparatus equipped with Waters RH columns and a Dawn Eos (Wyatt Technology) multiangle laser light scattering detector and the measurements were carried out at 25 °C with tetrahydrofuran (THF) as the eluent at the rate of 1.0 mL/min.

Atomic Force Microscopy (AFM). The specimens of thermosets for AFM observation were trimmed using an ultrathin microtome machine, and the thickness of the specimens was about 70 nm. The morphological observation of the specimens was conducted on a Nanoscope IIIa scanning probe microscope (Digital Instruments, Santa Barbara, CA) in tapping mode. A tip fabricated from silicon (125 μm in length with *ca.* 500 kHz resonant frequency) was used for scan, and the scan rate was 2.0 Hz.

Small-Angle X-ray Scattering (SAXS). The SAXS measurements were taken on a small-angle X-ray scattering station (BL16B1) with a long-slit collimation system in the Shanghai Synchrotron Radiation Facility (SSRF), Shanghai, China, in which the third generation of synchrotron radiation light sources was employed. Two dimensional diffraction patterns were recorded using an image intensified CCD detector. The experiments were carried out with the radiation of X-ray with the wavelength of λ = 1.24 Å at room temperature (25 °C). The intensity profiles were output as the plot of scattering intensity (I) versus scattering vector, $q = (4\pi/\lambda) \sin(\theta/2)$ (θ = scattering angle).

Dynamic Mechanical Thermal Analysis (DMTA). Dynamic mechanical tests were carried out on a TA Instruments DMA Q800 dynamic mechanical thermal analyzer (DMTA) equipped with a liquid nitrogen apparatus in a single cantilever mode. The frequency used was 1.0 Hz, and the heating rate of 3.0 °C/min was used. The specimen dimension was 25 × 5.0 × 1.75 mm^3. The experiments were carried out from −80 to +250 °C.

Phase Contrast Microscopy (PCM). A Leica DMLP polarized optical microscope equipped with a hot stage (Linkam TH960, Linkam Scientific Instruments, Ltd., U.K.) with a precision of ±0.1 °C was used for the determination of onset of reaction-induced phase separation for DGEBA-DDS and PS (and/or PCL) mixtures. Typically, tetrahydrofuran solutions of the mixtures were cast onto cover glasses; the majority of solvent was removed at room temperature and the residual solvent was further eliminated *in vacuo* at 30 °C for 2 h. The films of the blends were sandwiched between two cover glasses. The blend films were observed under the polarizing microscope in which the angle between the polarizer and analyzer was 45°.[51] The samples were rapidly heated up to 150 °C to record the evolution of micrograph at this temperature as a function of curing time. The micrographs were automatically recorded with an interval of 30 s with a Sony Hyper HAD digital color video camera until the morphology becomes no longer changed. The images were analyzed by using a public domain image processing and analysis program freely available from the National Institutes of Health USA (Image J)[52] to obtain the plot of particle area fraction as a function of curing time.

Isothermal Curing Behavior. The equimolar mixture of DGEBA, PEO with DDS and the model PS (and/or PCL) were dissolved in a smallest amount of tetrahydrofuran at room temperature. The majority of solvent was removed via rotary evaporation at room temperature and the mixture was further desiccated in a vacuum oven at 30 °C for 4 h to eliminate the residual solvent. The isothermal curing behavior was investigated by means of differential scanning calorimetry (DSC). First, the sample (about 5 mg in weight) was rapidly heated up to 150 °C and the isothermal endothermic enthalpy was recorded as a function of time. The conversion of isothermal endothermic enthalpy [$\alpha(t)$] as a function of curing time (t) was determined using the following equation:

$$\alpha(t) = \int_{t_0}^{t} \left(\frac{dH}{dt}\right) dt \Big/ \int_{t_0}^{\infty} \left(\frac{dH}{dt}\right) dt \quad (1)$$

Here t_0 is the time at which the sample reaches isothermal conditions, as indicated by a flat baseline after an initial spike in the thermal curves. The integral in the numerator is the enthalpy generated during the time $t - t_0$, and the integral in the denominator is the total enthalpy of curing.

RESULTS AND DISCUSSION

Synthesis of PEO-*b*-PCL-*b*-PS Triblock Copolymer. The synthesis route of poly(ethylene oxide)-*block*-poly(ε-caprolactone)- *block*-polystyrene (PEO-*b*-PCL-*b*-PS) triblock copolymer is shown in Scheme 1. In the first step, a monohydroxyl-terminated poly(ethylene oxide)-*block*-poly(ε-caprolactone) diblock copolymer was obtained via ring-opening polymerization of ε-caprolactone with poly(ethylene oxide) monomethyl ether (MPEO5000) with a quoted molecular weight of M_n = 5,000 as the macromolecular initiator and stannous(II) octanoate [$Sn(Oct)_2$] as the catalyst. The monohydroxyl-terminated diblock copolymer (denoted PEO-*b*-PCL−OH) was used to react with 2-bromoisobutyryl bromide in the presence of triethylamine to obtain 2-bromoisobutyryl-terminated PEO-*b*-PCL

Scheme 1. Synthesis of PEO-*b*-PCL-*b*-PS Triblock Copolymer

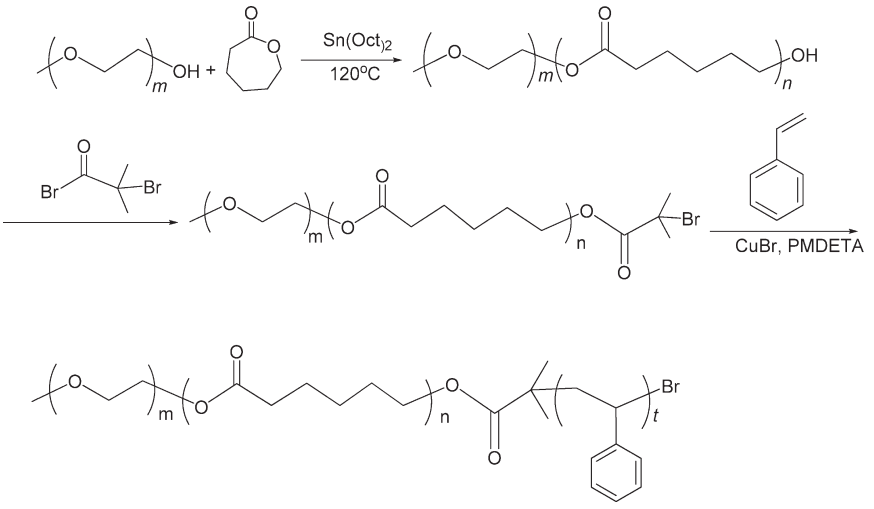

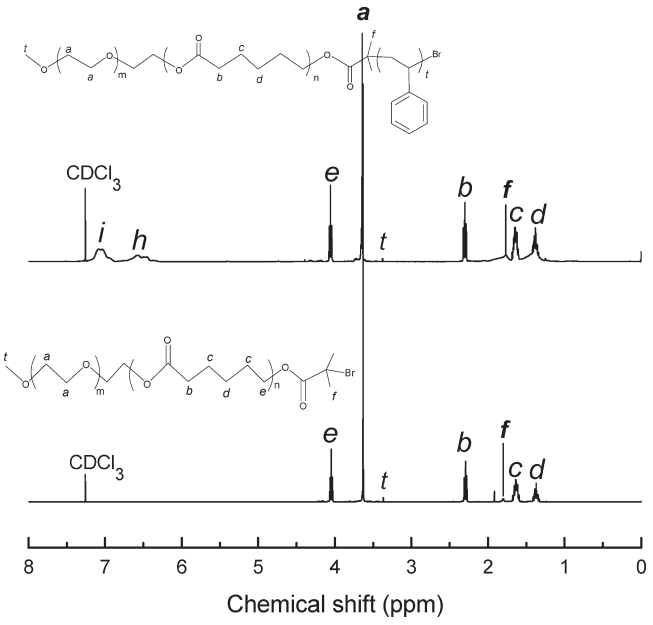

Figure 1. ^{1}H NMR spectra of PEO-*b*-PCL diblock and PEO-*b*-PCL-*b*-PS triblock copolymers.

[PEO-*b*-PCL−OOCC$(CH_3)_2$Br], which was then used as the macromolecular initiator for atom transfer radical polymerization of styrene to afford the PEO-*b*-PCL-*b*-PS ABC triblock copolymer. Shown in Figure 1 are the ^{1}H NMR spectra of monohydroxyl-terminated PEO-*b*-PCL diblock and PEO-*b*-PCL-*b*-PS triblock copolymers. For the PEO-*b*-PCL diblock copolymer, the sharp single peak of resonance centered at 3.63 ppm is attributed to methylene protons of PEO and the resonance signals at 4.03, 2.28, 1.61, and 1.36 are assigned to methylene protons of PCL block. The signal assignable to the protons of terminal methoxyl group of MPEO5000 appeared at 3.38 ppm, and the resonance of methyl groups from 2-bromoisobutyryl moiety at the end of PCL block appeared at 1.81 ppm. The ^{1}H NMR spectroscopy indicates that the product combined the structural features from PEO and PCL and the terminal hydroxyl

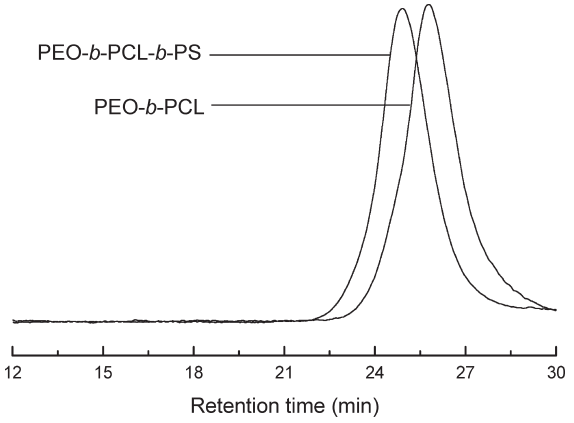

Figure 2. GPC curves of PEO-*b*-PS diblock and PEO-*b*-PCL-*b*-PS triblock copolymers.

groups were successfully capped with 2-bromoisobutyryl groups. For the PEO-*b*-PCL-*b*-PS ABC triblock copolymer, the resonance of protons of aromatic rings was detected in the range of 6.3−7.3 ppm besides the signals of resonance assignable to PEO-*b*-PCL diblock copolymer. The ^{1}H NMR spectroscopy indicates that PS block was successfully connected onto the PEO-*b*-PCL diblock copolymer, i.e., the product possessed the structural features from PEO, PCL and PS. The above PEO-*b*-PCL diblock and PEO-*b*-PCL-*b*-PS triblock copolymers were subjected to gel permeation chromatography (GPC) to measure the molecular weights and the GPC profiles were presented in Figure 2. It is seen that the GPC curves displayed single and unimodal peaks, suggesting that no homopolymers and poly(ethylene oxide) monomethyl ether were detected. For the PEO-*b*-PCL diblock copolymer, the molecular weight was measured to be M_n = 13 160 with M_w/M_n = 1.10. For the PEO-*b*-PCL-*b*-PS triblock copolymer, the molecular weight was measured to be M_n = 21,046 with M_w/M_n = 1.06. The results of ^{1}H NMR spectroscopy and GPC indicate that the PEO-*b*-PCL-*b*-PS ABC triblock copolymer was successfully obtained.

Nanostructures of Epoxy Thermosets Containing PEO-*b*-PCL-*b*-PS. The PEO-*b*-PCL-*b*-PS triblock copolymer was

dx.doi.org/10.1021/ma201456x |*Macromolecules* 2011, 44, 8546–8557

incorporated into epoxy to access the nanostructures in the thermosets. In this work, 4,4′-methylenebis(2-chloroaniline) (MOCA) and 4,4′-diaminodiphenylsulfone (DDS) were respectively used as the hardeners to obtain the thermosets. Before curing, all the mixtures composed of DGEBA, MOCA (and/or DDS) and PEO-*b*-PCL-*b*-PS were homogeneous and transparent at room and elevated temperatures. The results of small-angle X-ray scattering showed that no self-organized nanophases were formed in the ternary mixtures of DGEBA, the hardener (i.e., MOCA or DDS) and the triblock copolymer at room and elevated temperatures. After cured at elevated temperature the thermosets with the content of PEO-*b*-PCL-*b*-PS triblock copolymer up to 40 wt % were obtained. All the epoxy thermosets containing PEO-*b*-PCL-*b*-PS triblock copolymer were homogeneous and transparent, suggesting that no macroscopic phase separation occurred in the process of curing reaction. The morphologies of the thermosets was investigated by means of atomic force microscopy and small-angle X-ray scattering, respectively.

MOCA-Cross-Linked Thermosets. In order to investigate the nanostructures, the as-prepared thermosets were trimmed using an ultrathin microtome machine and the sections of the samples were subjected to the morphological observation by means of atomic force microscopy (AFM). For the MOCA-cured thermosets, the AFM micrographs were presented in Figure 3. The left and right images are the topography and phase contrast images, respectively. In all the cases, the epoxy thermosets containing PEO-*b*-PCL-*b*-PS triblock copolymer displayed microphase-separated morphologies. In views of the weight fraction of the triblock copolymer in the thermosets and the miscibility of the copolymer subchains with MOCA-cross-linked epoxy, it is judged that the dispersed microdomains are attributed to PS blocks. The spherical PS nanophase were dispersed in the continuous epoxy matrix until the content of the diblock copolymer is 30 wt %. For the thermoset containing 10 wt % PEO-*b*-PCL-*b*-PS triblock copolymer, the uniform nanodomains with the size of 10−20 nm were dispersed in the continuous epoxy matrix (Figure 3A). With increasing content of the triblock copolymer, some PS microdomains became interconnected and the worm-like PS microdomains began to appear until the content of PEO-*b*-PCL-*b*-PS triblock copolymer attained 30 wt % and the order of the nanostructures increased with increasing content of PEO-*b*-PCL-*b*-PS triblock copolymer (see Figure 3, parts b and c). While the content of the triblock copolymer was 40 wt %, an ordered nanostructure was displayed as shown in Figure 3d. According to the AFM micrograph, it is plausible to propose that the spherical PS microdomains were arranged into a kind of cubic lattice, which will be further determined by means of small-angle X-ray scattering (SAXS)

The SAXS profiles of the nanostructured thermosets containing PEO-*b*-PCL-*b*-PS triblock copolymer were showed in Figure 4. In all the cases the multiple scattering peaks were displayed. For the thermoset containing 10 wt % PEO-*b*-PCL-*b*-PS triblock copolymer the primary intense scattering peak was detected at q = 0.19 nm^{-1} and another weak scattering was discernible at q = 0.34 nm^{-1}. The intensity of higher-order scattering peaks increased with increasing the content of PEO-*b*-PCL-*b*-PS triblock copolymer. By simulating the SAXS profiles, it was found that the higher-order scattering peaks appeared at the q values of $3^{1/2}$, $4^{1/2}$, and $7^{1/2}$ relative to the first-order scattering peak positions (q_m) while the content of PEO-*b*-PCL-*b*-PS triblock copolymer was 20 wt % or higher. The positions of the higher-order

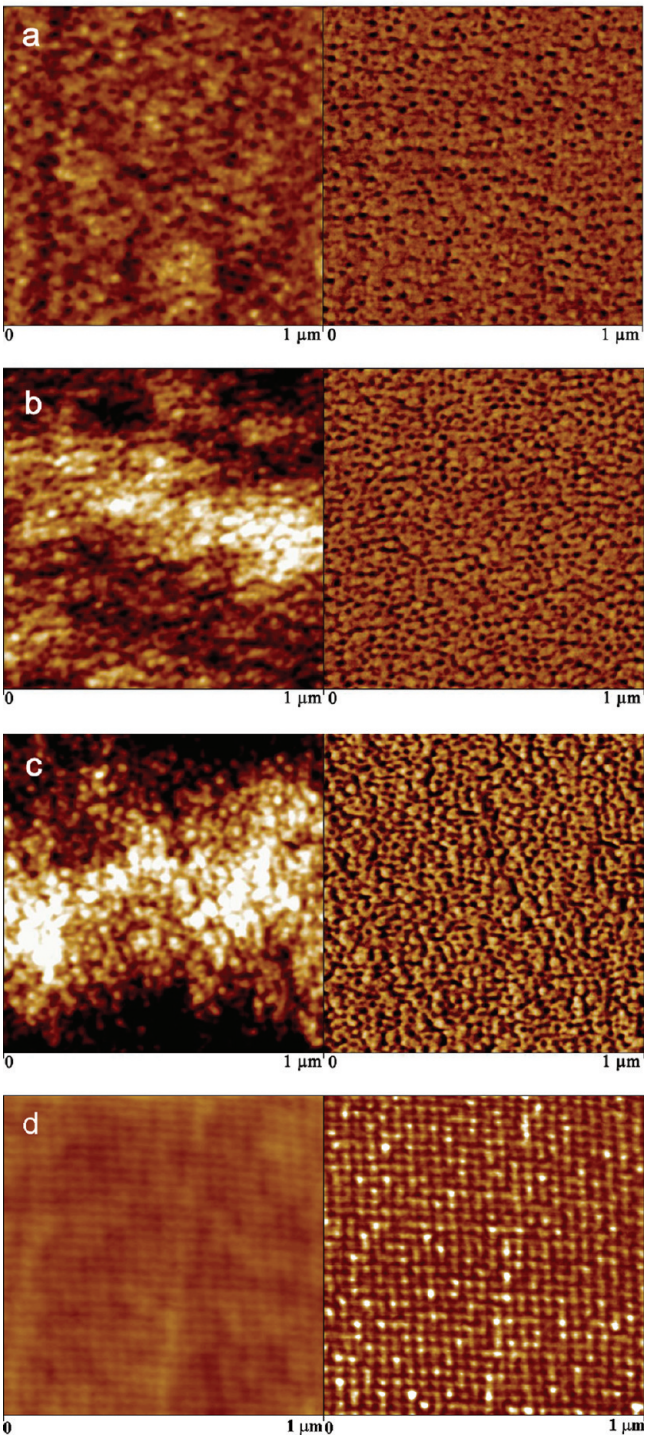

Figure 3. AFM images of epoxy thermosets containing (a) 10, (b) 20, (c) 30, and (d) 40 wt % of PEO-*b*-PCL-*b*-PS triblock copolymer with MOCA as hardener. Left: height image. Right: phase contrast image.

scattering peaks correspond to the nanostructure that the PS nanodomains in the thermosetting matrix were arranged into body-centered cubic (*bcc*) lattice. According to the positions of the first-order scattering peaks, the Bragg's spacing d_m can be obtained to be 33.9, 30.2, 29.7, and 29.5 nm for the thermosets containing 10, 20, 30, and 40 wt % PEO-*b*-PCL-*b*-PS triblock copolymer, respectively. The results of SAXS indicate that while MOCA was used as the hardener, the spherical PS nanophases

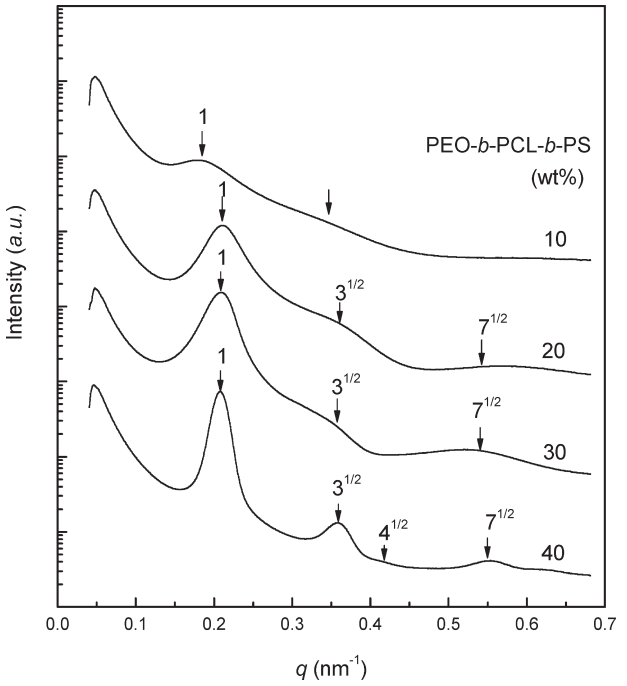

Figure 4. SAXS profiles of the epoxy thermosets containing PEO-*b*-PCL-*b*-PS triblock copolymer with MOCA as hardener.

were formed in the thermosets, which were arranged into body-centered cubic (*bcc*) lattice although the ordering was not sufficiently strong.

DDS-Cross-Linked Thermosets. The AFM micrographs of the epoxy thermosets with DDS as the hardener are shown in Figure 5. It is seen that all the thermosets containing PEO-*b*-PCL-*b*-PS triblock copolymer displayed microphase-separated morphologies. Nonetheless, the nanostructures were apparently different from the counterparts cured with MOCA. For the thermosets containing the PEO-*b*-PCL-*b*-PS triblock copolymer of 20 wt % or less, the spherical nanodomains were dispersed in the continuous epoxy matrix. The size of the spherical nanophase was 20−30 nm and apparently higher than that in the MOCA-cross-linked thermosets (see Figure 5, parts a and b). While the content of PEO-*b*-PCL-*b*-PS triblock copolymer is 30 wt % or higher, the thermosets displayed lamellar nanostructures (Figures 5c and 5d), which was in marked contrast to those in the counterparts with MOCA as the hardener. In the lamellar nanostructures, the thickness of each nanolayer was 40 nm. Careful observation showed that each nanolayer in the nanostructured thermosets was not homogeneous in composition and could be composed of both PS and PCL blocks.

The above nanostructures were further investigated by means of small-angle X-ray scattering (SAXS) and the profiles of the SAXS are presented in Figure 6. While the thermoset contained 10 wt % PEO-*b*-PCL-*b*-PS triblock copolymer a single and broad scatter peak appeared at q = 0.20 nm^{-1}, suggesting that the thermoset was microphase-separated and the nanostructure was disordered. While the content of PEO-*b*-PCL-*b*-PS triblock copolymer is 20 wt % or higher the multiple scattering peaks were detected as indicated with arrows in Figure 6. According to the position of the higher-order scattering peaks relative to the first-order scattering peaks, it is judged that the nanophases in the thermoset containing 20 wt % triblock copolymer could be

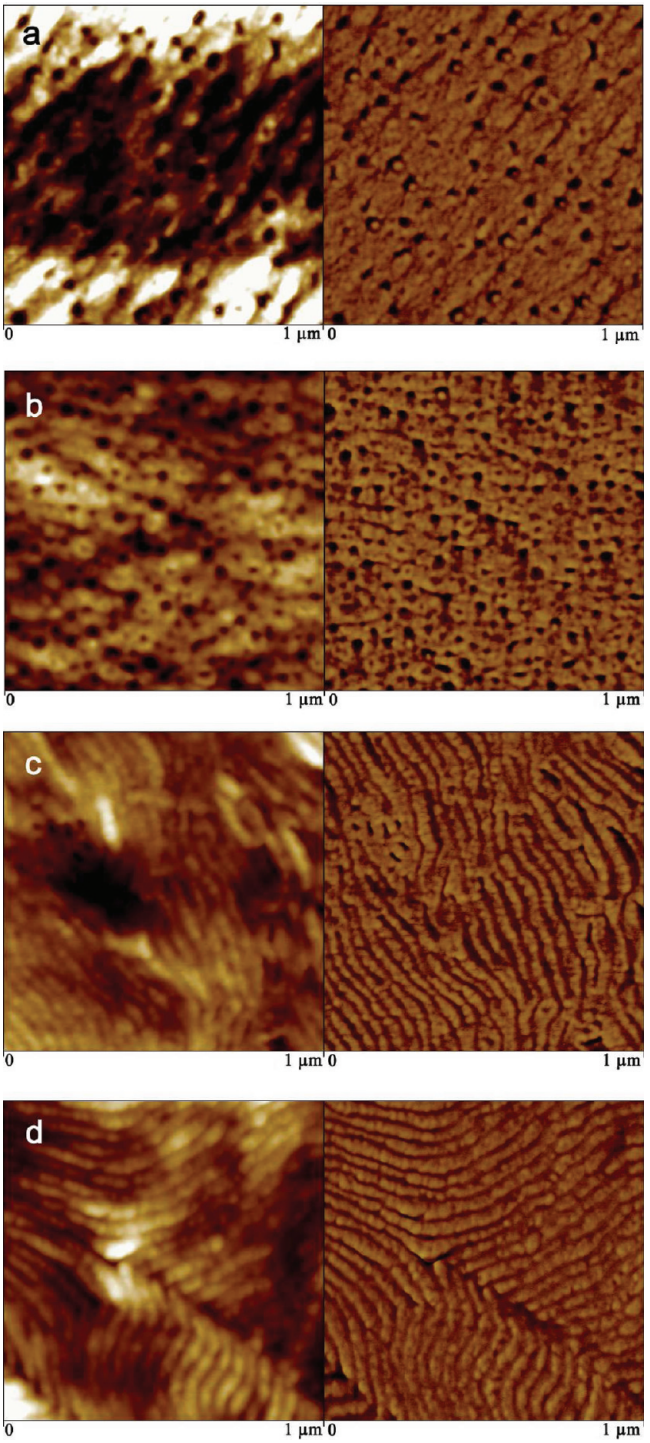

Figure 5. AFM images of epoxy thermosets containing (A) 10, (B) 20, (C) 30, (D) 40 wt % of PEO-*b*-PCL-*b*-PS triblock copolymer with DDS as hardener. Left: height image. Right: phase contrast image.

arranged into body- (or face-) centered cubic lattice. It should be pointed out that it is not easy unambiguously to judge the types of packing lattices only in terms of SAXS profiles for the thermoset containing 20 wt % PEO-*b*-PCL-*b*-PS since the scattering peaks were quite broad; i.e., the ordering was apparently not good enough. While the contents of PEO-*b*-PCL-*b*-PS triblock copolymer are 30 and 40 wt %, the nanodomains were arranged into lamellar lattices. According to the positions of the

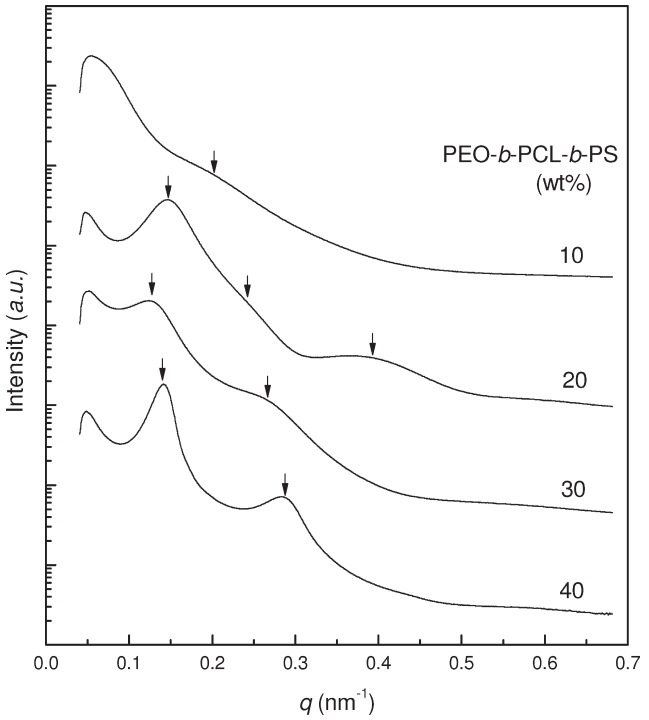

Figure 6. SAXS profiles of the epoxy thermosets containing PEO-*b*-PCL-*b*-PS triblock copolymer with DDS as hardener.

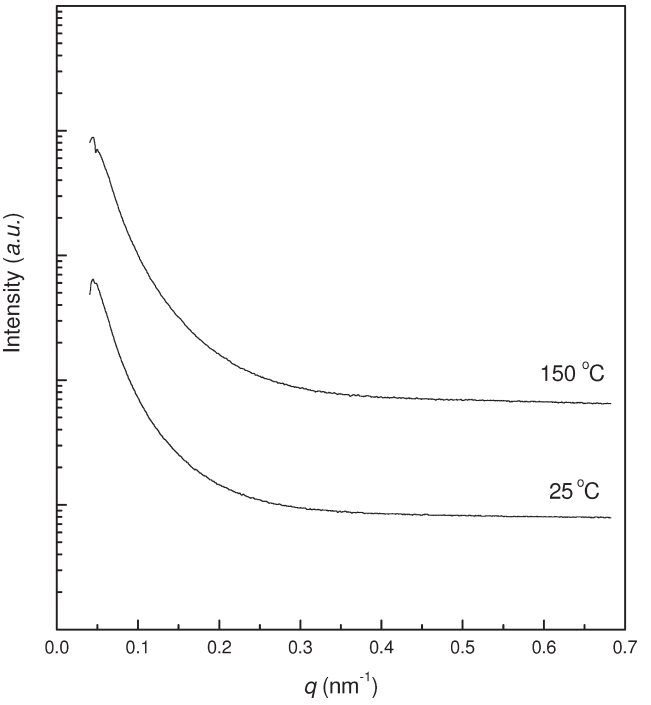

Figure 7. SAXS profiles of the mixture of DGEBA, MOCA, and 10 wt % PEO-*b*-PCL-*b*-PS triblock copolymer at 25 and 150 °C, respectively.

first-order scattering peaks, the Bragg's spacing d_m can be obtained to be 30.4, 41.3, 47.2, and 43.6 nm for the thermosets containing 10, 20, 30, and 40 wt % PEO-*b*-PCL-*b*-PS triblock copolymer, respectively. This SAXS results were in a good agreement with those by AFM.

Interpretation of Nanostructure Formation. It has been indentified that the formation of nanostructures in thermosets containing block copolymers could follow either self-assembly[1,2] or reaction-induced microphase separation[7,8] mechanism. In the present case, the formation mechanism of nanostructures was investigated by means of small-angle X-ray scattering. Representatively shown in Figures 7 and 8 are the SAXS profiles of the mixtures of epoxy precursors and 10 wt % PEO-*b*-PCL-*b*-PS triblock copolymer before curing reaction. For the system with MOCA as the hardener, no scattering peaks were detected at room temperature and the curing temperature (i.e., 150 °C) (see Figure 7), implying that no self-assembled nanophases were formed. For the system with DDS as the hardener, the situation was slightly different. At room temperature, two broad scattering peaks were discernible at *ca.*, q = 0.11 and 0.23 nm^{-1}, suggesting that the triblock copolymer was self-assembled into nanophases in the mixture with the epoxy precursors. Upon heating the system to the curing temperature, the scattering peaks disappeared (see Figure 8), suggesting that the self-organized nanophases no longer existed due to the upper critical solution temperature (UCST) behavior of PS block in the mixture with the epoxy precursors.[44,45] Nonetheless, the results of SAXS showed that the mixtures composed of the epoxy precursors and PEO-*b*-PCL-*b*-PS triblock copolymer were homogeneous at the beginning of the curing reaction. Therefore, it is judged that the formation of nanostructures in the thermosets containing PEO-*b*-PCL-*b*-PS triblock copolymer followed reaction-induced microphase separation rather than self-assembly mechanism. It is

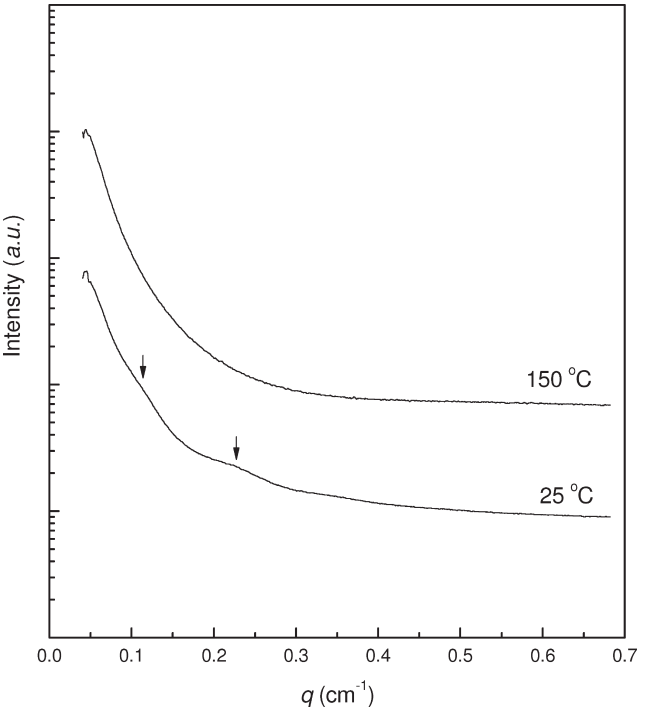

Figure 8. SAXS profiles of the mixture of DGEBA, DDS, and 10 wt % PEO-*b*-PCL-*b*-PS triblock copolymer at 25 and 150 °C, respectively;.

noted that the nanostructures in the epoxy thermosets containing PEO-*b*-PCL-*b*-PS triblock copolymer were quite dependent on the type of hardeners. The morphological transition induced by different hardeners could be interpreted in terms of: (i) hardener-dependent miscibility of the ABC terpolymer blocks

with epoxy thermosets and (ii) occurrence of tandem reaction-induced microphase separation.

Hardener-Dependent Miscibility of Copolymer Blocks with Epoxy. It is critical to know the miscibility of the copolymers blocks (i.e., PEO, PCL and PS) with epoxy while MOCA or/and DDS was used as the hardener for understanding the formation of nanostructures in the present epoxy thermosets containing PEO-*b*-PCL-*b*-PS triblock copolymer. The thermosetting blends of epoxy thermosets with PEO are among the most investigated systems and the miscibility of the blends has been established by several groups.[39−43] Woo et al.[41] have reported that the blends of epoxy with PEO are miscible while DDS was used as the hardener. Our previous investigations[43] showed that the blends were also miscible while MOCA was used as the hardener. The miscibility has been ascribed to the formation of the strong intermolecular hydrogen bonding interactions between hydroxyl ether units of amine-cross-linked epoxy and ether oxygen atoms of PEO. For the binary blends of epoxy with PS, the reaction-induced microphase separation always occurs, irrespective of hardeners.[44,45] Nonetheless, the miscibility of epoxy and PCL blends was quite dependent on types of hardeners.[46] It has been found that the blends were miscible after and before curing reaction while MOCA was used as the hardener.[43,49] The miscibility is attributed to the formation of the interchain hydrogen bonding interactions between hydroxyl ether structural units of epoxy thermoset and carbonyl groups of PCL. However, the reaction-induced microphase separation occurred while DDS was used as the hardeners although DDS is also diamine.[48,49] The previous results show that the intermolecular specific interactions (viz. hydrogen bonding) in the thermosetting blends of DDS-cross-linked epoxy with PCL were significantly weaker than those in the blends of epoxy with PCL with MOCA as the hardener. It was proposed that the presence of considerable intramolecular hydrogen bonds between sulfonyl groups from DDS moieties and hydroxyl ether structural units of epoxy networks could significantly suppress the formation of the strong intermolecular hydrogen bonding interactions between carbonyls and hydroxyl ether structural units of epoxy networks and thus the reaction-induced phase separation takes place.[49] It should be pointed out that besides the intermolecular (and/or intramolecular) specific interactions, the dependence of the miscibility of epoxy thermosets with PCL on the hardeners could be related to the difference in solubility parameters for the two thermosetting systems.

The dependence of miscibility in the blends of epoxy with PCL on hardeners could be employed to modulate the nanostructures in epoxy thermosets containing PEO-*b*-PCL-*b*-PS triblock copolymer by the use of different hardeners. It is anticipated that while MOCA is used as the hardener only PS nanophases are formed whereas both PEO and PCL blocks remain miscible with epoxy−MOCA networks. While DDS is used as the hardener, both PS and PCL blocks would be demixed out of epoxy matrix and form the microdomains. The demixing of the blocks (viz. PS or/and PCL) in the nanostructured thermosets can be readily investigated by means of dynamic mechanical thermal analysis (DMTA). Shown in Figures 9 and 10 are the DMTA curves for the thermosets while MOCA and DDS were used as the hardener, respectively. For the MOCA-cross-linked thermosets, the control epoxy exhibited a well-defined α transition centered at *ca.* 159 °C, which corresponds to the glass−rubber transition of the cross-linked polymer (See Figure 9). For the nanostructured thermosets containing PEO-*b*-PCL-*b*-PS triblock copolymer, the T_α of PS microdomains was detected at *ca.* 65 °C besides the α transitions assignable to epoxy matrix. It is seen that the T_α's of PS microdomains remained invariant, irrespective of the concentration of the triblock copolymer but the T_α's of epoxy matrices decreased with increasing the content of PEO-*b*-PCL-*b*-PS triblock copolymer. The appearance of T_α's assignable to PS microdomains indeed indicates that PS blocks were demixed out of epoxy matrices. The observation that no major transitions assignable to PEO (or PCL) were detected indicates that both PEO and PCL blocks remained mixed with epoxy matrices. The decreased T_α's for epoxy matrices is ascribed to the plasticization of both PEO and PCL blocks which possessed a lower T_g (i.e., −65 °C) on epoxy-MOCA networks. For the DDS-cross-linked thermosets, the control epoxy exhibited the T_α of 199 °C (see Figure 10) and a β relaxation was detected at −25 °C, which could be associated with the hydroxyl ether structural units [i.e., $-O-CH_2-CH(OH)-CH_2-O-$].[53−55] It is noted that the DMTA thermograms of the DDS-cross-linked thermosets were more complicated than those of the counterparts cured with MOCA. The nanostructured thermoset containing 10 wt % of PEO-*b*-PCL-*b*-PS triblock copolymer displayed two major transitions at *ca.*195 and 64 °C, respectively. The former corresponds to the glass transition of epoxy−DDS network which were mixed with PEO blocks whereas the latter could be related to the nanodomains dispersed in the matrix, which could be composed of PS and PCL blocks. It is noted that both major transitions were split into two components while the content of PEO-*b*-PCL-*b*-PS triblock copolymer is 20 wt % or higher. For the glass transition assignable to epoxy matrix, one component possessed the T_α's of *ca.* 198 °C, which are quite close to that of the control epoxy whereas the T_α's for another component decreased with increasing the content of PEO-*b*-PCL-*b*-PS triblock copolymer. The splitting of the major transitions could reflect the presence of compositional gradient in the epoxy matrix. It is proposed that the epoxy matrix close to the surface of the dispersed microdomains composed of PCL and PS were mixed with PEO blocks and thus possessed the lower T_α's whereas that far from the surface of the dispersed microdomains remained unmixed with PEO blocks and had the T_α's as high as the control epoxy. For the transition assignable to the dispersed microdomains, the separated peaks could be associated with the glass transitions of the combined microdomains from PCL and PS blocks. The components at the higher temperature (*ca.* 65 °C) are ascribed to the glass transition of PS blocks whereas those at the lower temperature (*ca.* 27 °C) are related to the PCL blocks, which is responsible for either melting or glass transition of PCL blocks. If any, the melting transition should be able to detect by wide-angle X-ray diffraction (XRD) and differential scanning calorimetry (DSC). The XRD results showed that there is no any crystallinity in the nanostructured thermosets. In the DSC profiles, there were also no detectable exothermic transitions responsible for the melting of PCL although the samples have been annealed at 25 °C for more than one month. Therefore, this transition cannot be ascribed to the melting transition of PCL microdomains. This peak could be attributed to the glass transition of PCL-rich microdomains. Nonetheless, a question arises why the T_g of PCL microdomains was much higher than T_g of normal PCL (viz. −65 °C). The enhanced T_g's for the PCL microdomains could be interpreted on the basis of the following aspects. First, the demixing of PCL blocks out of epoxy-amine phase could not undergo to completion due to the PCL block was not sufficiently long (viz. length = 8160 Da). As a

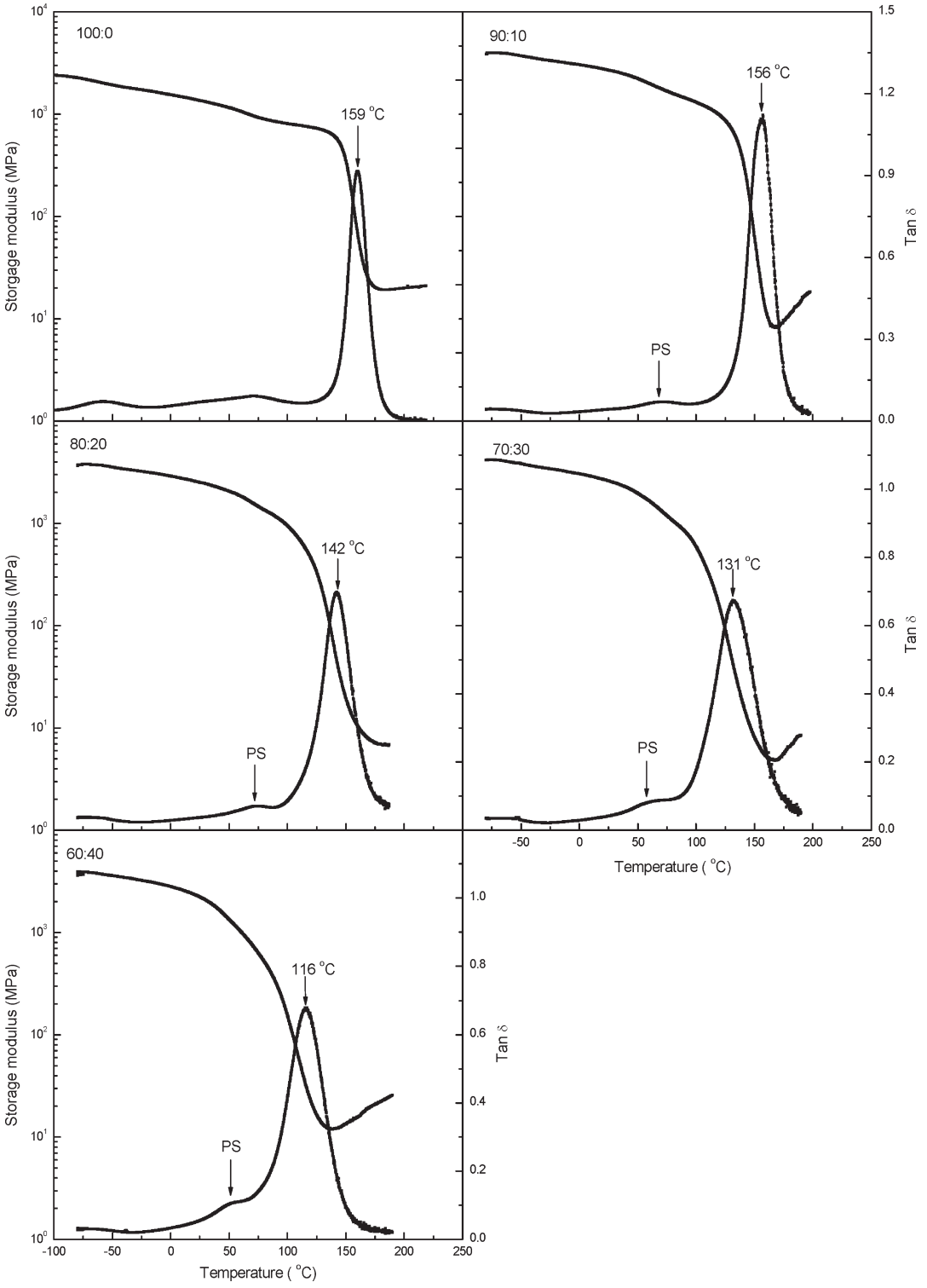

Figure 9. Dynamic mechanical spectra of the nanostructured epoxy thermosets cured with MOCA.

consequence, a small amount of epoxy was still remained in the PCL microdomains. Another possible explanation is that the PCL chains in the PCL microdomains were greatly restricted between two rigid microphases (viz. epoxy matrix and PS) and the PCL chains were significantly reinforced by epoxy matrix and PS microdomains. The above factors resulted in the enhanced T_g's for the PCL microdomains.

Tandem Reaction-Induced Microphase Separation. While MOCA was used as the hardener, PS block of PEO-*b*-PCL-*b*-PS triblock copolymer was demixed out of epoxy-amine phase as the spherical nanophases whereas both PEO and PCL blocks remained miscible with epoxy. This case quite resembles the reaction-induced microphase separation in epoxy thermosets containing AB diblock copolymers such as PEO-*b*-PS[8] or

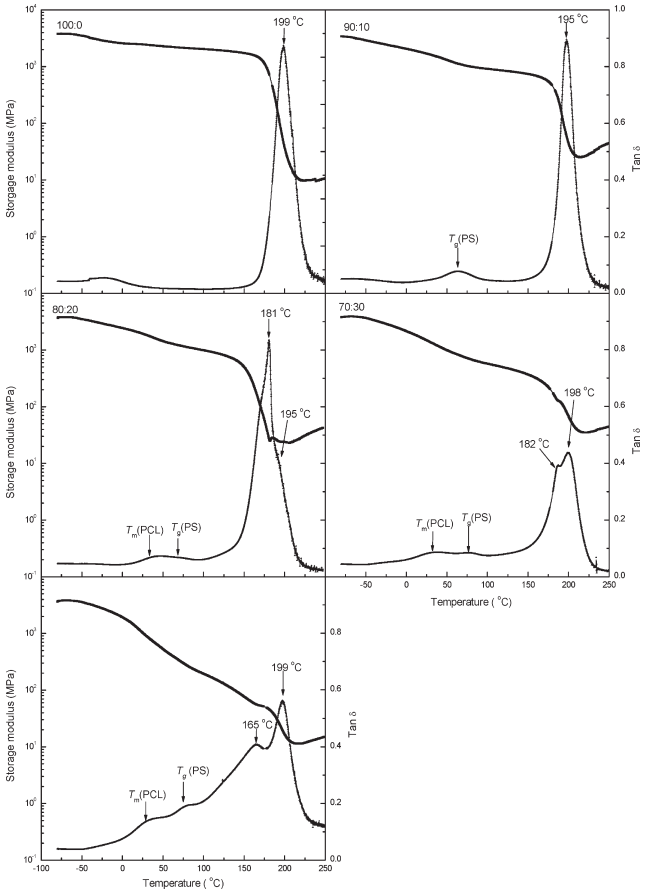

Figure 10. Dynamic mechanical spectra of the nanostructured epoxy thermosets cured with DDS.

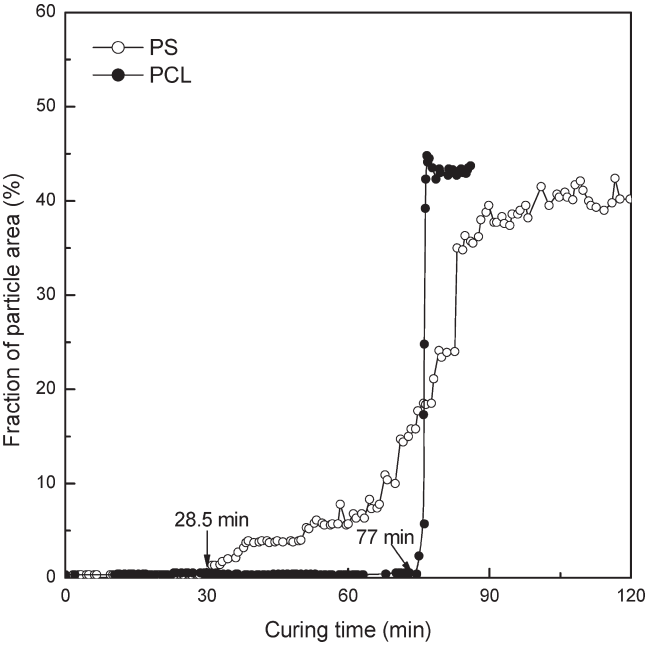

Figure 11. Plots of domain area fraction of the model PS of 17.73 wt % and the model PCL of 18.24 wt % as functions of curing time at 150 °C.

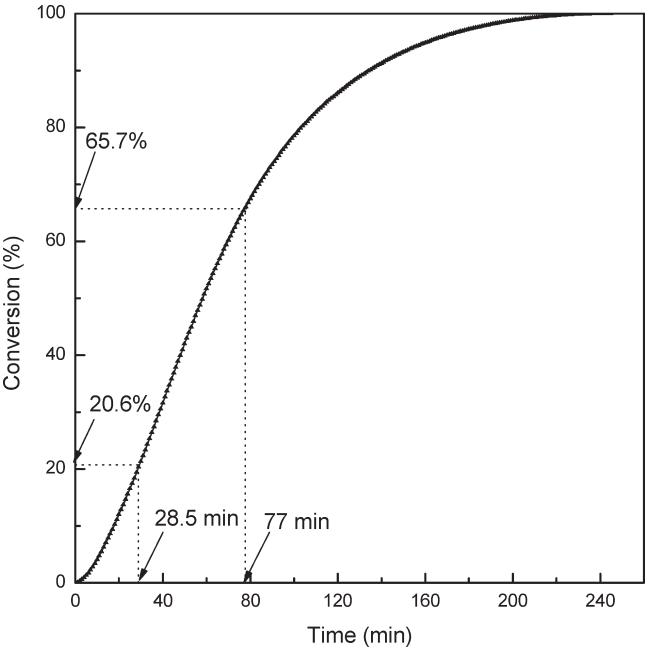

Figure 12. Plot of conversion for the blends of epoxy containing 40% PEO-*b*-PCL-*b*-PS triblock copolymer cured at 150 °C.

PCL-*b*-PS[31] although the ABC triblock copolymer was used. It was found that the PS spherical nanophases were arranged into the nanostructures with body-centered cubic (*bcc*) lattice while the content of the terpolymer is 20% or more in terms of the results of AFM and SAXS (see Figures 3 and 4). While DDS was used as the hardener, both PS and PCL blocks were demixed out whereas PEO block remained mixed with the epoxy matrix. The results of AFM and SAXS shows that the nanophases composed of PS and PCL were arranged into lamellar lattices while the content of PEO-*b*-PCL-*b*-PS triblock copolymer was 30 w% or higher. Nonetheless, a question arises whether the PS and PCL blocks were demixed out of epoxy-amine phase in simultaneous (or tandem) fashion. It is helpful to know this question for understanding the formation of the lamellar nanostructures in the thermosets containing PEO-*b*-PCL-*b*-PS triblock copolymer. To examine the relative rates of microphase separation of the both immiscible blocks (viz. PCL and PS) in epoxy, we investigated the kinetics of reaction-induced phase separation in the blends of epoxy with the model PEO, PCL and PS homopolymers by means of optical microscopy and differential scanning calorimetry (DSC). The model homopolymers possessing the identical molecular weights with the lengths of the corresponding subchains in the PEO-*b*-PCL-*b*-PS triblock copolymer were utilized. The mixtures composed of the precursors of epoxy (DGEBA + DDS), PEO and the model PCL (and/or PS) were subjected to phase-contrast microscopy at the curing temperature (i.e., 150 °C) and the onset of reaction-induced phase separation was judged on the basis of the change of transmittance as a function of curing time. The phase-separated micrographs were analyzed by using a domain image analysis program[52] to obtain the fraction of demixed domains. Representatively shown in Figure 11 are the plots of domain area fraction as functions of curing time for the epoxy blend containing 17.73 wt % PS and/or 18.24 wt % PCL, which corresponds to the contents of PCL and/or PS in the nanostructured thermoset containing 40 wt % of PEO-*b*-PCL-*b*-PS triblock copolymer. It is seen that the domain area of the blends remained invariant for a long time after the

Scheme 2. Formation of Spherical and Lamellar Nanophases in Epoxy Thermosets Containing PEO-*b*-PCL-*b*-PS Triblock Copolymer

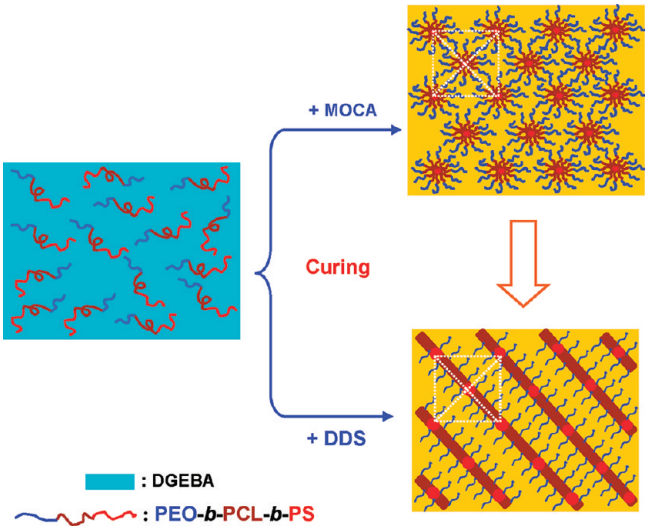

curing reaction was initiated. The phase separation induced by reaction was detected as indicated by the abrupt increase in domain area fraction. For the blend of epoxy with the model PS of 17.73 wt % the onset time of the phase separation was determined to be *ca.* 29 min. For the blend of epoxy containing the model PCL the onset of phase separation occurred at *ca.* 77 min. It is noted that the demixing of PCL out of epoxy matrix was much later than PS, suggesting that the RIMPS of PS and PCL blocks in the thermosetting blends containing PEO-*b*-PCL-*b*-PS triblock copolymer could be in a tandem manner other than a simultaneous fashion. It is seen that the phase separation of the model PS was almost completed at *ca.* T_{end} = ~77 min, at which the demixing of PCL was just started. The fact that the demixing for PCL block was earlier than that of PS block could result from the intermolecular interaction parameter (χ) in the epoxy and PS blends higher than that in the epoxy and PCL blends, which can be estimated according to solubility parameters.[56] By measuring the isothermal curing kinetics by means of DSC, the demixing of PS and PCL corresponded to the conversion of epoxy monomers to be 20.6 and 65.7%, respectively (see Figure 12). According to Flory−Stockmayer's theory,[57,58] the conversion at gel (viz. gel point) for the mixture of DGEBA and DDS was calculated to be *ca.* 57.7%. If the difference in reaction activity between primary and secondary amines is considered, it is generally accepted that the conversion at gel for the mixture of DGEBA with DDS is in the range of 58−62%.[59,60] The both conversions at gel point were significantly lower than the value of 65.7%, suggesting that the demixing of PCL blocks could undergo in a restricted manner owing to the formation of the cross-linked network. It is proposed that the demixing of PCL block s could be taken as s secondary microphase separation after the gel point.[61] It is proposed that PS blocks were first demixed from epoxy-DDS phase in the form of spherical nanophases and the subsequent demixing of PCL blocks occurred around the spherical PS nanodomains owing to the connectivity of PCL midblock with PS end blocks. When the content of PEO-*b*-PCL-*b*-PS triblock copolymer is relatively low (*e.g.,* 20 wt % or less), the PS subchains could be demixed into separate spherical particles, which were surrounded by the PCL nanolayers (see Figure 5, parts a and b). With increasing the concentration of PEO-*b*-PCL-*b*-PS, the composite nanophases composed of PS and PCL blocks became interconnected (see Figure 5, parts c and d) owing to the increased volume fraction for the separate nanospheres. According to geometric calculation, the merge of the nanophases could preferentially occur at the shortest distance between adjacent spherical nanodomains (i.e., the distance between a vertex spherical nanodomain and its adjacent central nanodomain in a body-center cubic cell) and thus the lamellar nanophases were formed as depicted in Scheme 2. This observation could be taken as a morphological transition of ordered nanostructures from spherical to lamellar nanophases, which was induced by hardeners.

CONCLUSIONS

Poly(ethylene oxide)-*block*-poly(ε-caprolactone)-*block*-polystyrene triblock copolymer (PEO-*b*-PCL-*b*-PS) was synthesized via the combination of ring-opening polymerization (ROP) and atomic transfer radical polymerization (ATRP). The ABC triblock copolymer was incorporated into epoxy thermosets to access the nanostructures in the thermosets. The nanostructures of the epoxy thermosets can be modulated by the use of different hardeners. For the thermosets cured with 4,4′-methylenebis (2-chloroaniline) (MOCA), the long-ranged ordered nanostructures with body-centered cubic (*bcc*) lattice were obtained at the compositions investigated. While 4,4′-diaminodiphenylsulfone (DDS) was used as the hardener, the thermosets displayed the lamellar nanostructures. The formation of nanostructures in the thermosets have been evidenced by atomic force microscopy (AFM) and small-angle X-ray scattering (SAXS). The morphological transition from spherical to lamellar nanophase has been interpreted in terms of the hardener-dependent miscibility of the ABC terpolymer blocks with epoxy thermosets and the occurrence of tandem reaction-induced microphase separation.

AUTHOR INFORMATION

Corresponding Author

*Telephone: 86-21-54743278. Fax: 86-21-54741297. E-mail: szheng@sjtu.edu.cn.

ACKNOWLEDGMENT

Financial support from the Natural Science Foundation of China (No. 20774058, 50873059 and 51133003) and the National Basic Research Program of China (No. 2009CB930400) is gratefully acknowledged. The authors thank the Shanghai Synchrotron Radiation Facility for the support under Project Nos. 10sr0260 and 10sr0126.

REFERENCES

(1) Hillmyer, M. A.; Lipic, P. M.; Hajduk, D. A.; Almdal, K.; Bates, F. S. *J. Am. Chem. Soc.* **1997**, *119*, 2749.

(2) Lipic, P. M.; Bates, F. S.; Hillmyer, M. A. *J. Am. Chem. Soc.* **1998**, *120*, 8963.

(3) Zheng, S. *In Epoxy Polymers: New Materials and Innovations*; Pascault, J. P.; Williams, R. J. J., Eds.; Wiley-VCH: Weinheim, Germany, 2010; pp 79−108.

(4) Ruiz-Pérez, L.; Royston, G. J.; Fairclough, J. A.; Ryan, A. J. *Polymer* **2008**, *49*, 4475.

(5) Hu, D.; Xu, Z.; Zeng, K.; Zheng, S. *Macromolecules* **2010**, *43*, 2960.
(6) Amendt, M. A.; Chen, L.; Hillmyer, M. A. *Macromolecules* **2010**, *43*, 3924.
(7) Meng, F.; Zheng, S.; Zhang, W.; Li, H.; Liang, Q. *Macromolecules* **2006**, *39*, 711.
(8) Meng, F.; Zheng, S.; Li, H.; Liang, Q.; Liu, T. *Macromolecules* **2006**, *39*, 5072.
(9) Mijovic, J.; Shen, M.; Sy, J. W.; Mondragon, I. *Macromolecules* **2000**, *33*, 5235.
(10) Grubbs, R. B.; Dean, J. M.; Broz, M. E.; Bates, F. S. *Macromolecules* **2000**, *33*, 9522.
(11) Grubbs, R. B.; Dean, J. M.; Bates, F. S. *Macromolecules* **2001**, *34*, 8593.
(12) Guo, Q.; Thomann, R.; Gronski, W. *Macromolecules* **2002**, *35*, 3133.
(13) Ritzenthaler, S.; Court, F.; Girard-Reydet, E.; Leibler, L.; Pascault, J.-P. *Macromolecules* **2002**, *35*, 6245.
(14) Ritzenthaler, S.; Court, F.; Girard-Reydet, E.; Leibler, L.; Pascault, J.-P. *Macromolecules* **2003**, *36*, 118.
(15) Rebizant, V.; Abetz, V.; Tournihac, T.; Court, F.; Leibler, L. *Macromolecules* **2003**, *36*, 9889.
(16) Dean, J. M.; Verghese, N. E.; Pham, H. Q.; Bates, F. S. *Macromolecules* **2003**, *36*, 9267.
(17) Rebizant, V.; Venet, A. S.; Tournillhac, F.; Girard-Reydet, E.; Navarro, C.; Pascault, J.-P.; Leibler, L. *Macromolecules* **2004**, *37*, 8017.
(18) Dean, J. M.; Grubbs, R. B.; Saad, W.; Cook, R. F.; Bates, F. S. *J. Polym. Sci., Part B: Polym. Phys.* **2003**, *41*, 2444.
(19) Wu, J.; Thio, Y. S.; Bates, F. S. *J. Polym. Sci., Part B: Polym. Phys.* **2005**, *43*, 1950.
(20) Zucchi, I. A.; Galante, M. J.; Williams, R. J. J. *Polymer* **2005**, *46*, 2603.
(21) Thio, Y. S.; Wu, J.; Bates, F. S. *Macromolecules* **2006**, *39*, 7187.
(22) Serrano, E.; Tercjak, A.; Kortaberria, G.; Pomposo, J. A.; Mecerreyes, D.; Zafeiropoulos, N. E.; Stamm, M.; Mondragon, I. *Macromolecules* **2006**, *39*, 2254.
(23) Ocando, C.; Serrano, E.; Tercjak, A.; Pena, C.; Kortaberria, G.; Calberg, C.; Grignard, B.; Jerome, R.; Carrasco, P. M.; Mecerreyes, D.; Mondragon, I. *Macromelecules* **2007**, *40*, 4048.
(24) Maiez-Tribut, S.; Pascault, J.-P.; Soule, E. R.; Borrajo, J.; Williams, R. J. J. *Macromolecules* **2007**, *40*, 1268.
(25) Gong, W.; Zeng, K.; Wang, L.; Zheng, S. *Polymer* **2008**, *49*, 3318.
(26) Yi, F.; Zheng, S.; Liu, T. *J. Phys. Chem. B* **2009**, *113*, 11831.
(27) Meng, F.; Zheng, S.; Liu, T. *Polymer* **2006**, *47*, 7590.
(28) Sinturel, C.; Vayer, M.; Erre, R.; Amenitsch, H. *Macromolecules* **2007**, *40*, 2532.
(29) Ocando, C.; Serrano, E.; Tercjak, A.; Pena, C.; Kortaberria, G.; Calberg, C.; Grignard, B.; Jerome, R.; Carrasco, P. M.; Mecerreyes, D.; Mondragon, I. *Macromolecules* **2007**, *40*, 4068.
(30) Xu, Z.; Zheng, S. *Macromolecules* **2007**, *40*, 2548.
(31) Meng, F.; Xu, Z.; Zheng, S. *Macromolecules* **2008**, *41*, 1411.
(32) Fan, W.; Zheng, S. *Polymer* **2008**, *49*, 3157.
(33) Fan, W.; Wang, L.; Zheng, S. *Macromolecules* **2009**, *42*, 27.
(34) Ocando, C.; Tercjak, A.; Martín, M. D.; Ramos, J. A.; Campo, M.; Mondragon, I. *Macromolecules* **2009**, *42*, 6215.
(35) Fan, W.; Wang, L.; Zheng, S. *Macromolecule* **2010**, *43*, 10600.
(36) Serrano, E.; Larranaga, M.; Remiro, P. M.; Mondragon, I.; Carrasco, P. M.; Pomposo, J. A.; Mecerreyes, D. *Macromol. Chem. Phys.* **2004**, *205*, 987.
(37) Serrano, E.; Martin, M. D.; Tercjak, A.; Pomposo, J. A.; Mecerreyes, D.; Mondragon, I. *Macromol. Rapid Commun.* **2005**, *26*, 982.
(38) Hameed, N.; Guo, Q.; Xu, Z.; Hanley, T. L.; Mai, Y.-W. *Soft Matter* **2010**, *6*, 6119.
(39) Luo, X.; Zheng, S.; Zhang, N.; Ma, D. *Polymer* **1994**, *35*, 2619.
(40) Zheng, S.; Zhang, N.; Luo, X.; Ma, D. *Polymer* **1995**, *36*, 3609.
(41) Horng, T. J.; Woo, E. M. *Polymer* **1998**, *39*, 4115.
(42) Guo, Q.; Harrats, C.; Groeninckx, G.; Koch, M. H. J. *Polymer* **2001**, *42*, 4127.
(43) Yin, M.; Zheng, S. *Macromol. Chem. Phys.* **2005**, *206*, 929.
(44) Hoppe, C. E.; Galante, M. J.; Oyanguren, P. A.; Williams, R. J. J.; Girard-Reydet, E.; Pascault, J.-P. *Polym. Eng. Sci.* **2002**, *42*, 2361.
(45) Zucchi, I. A.; Galante, M. J.; Borrajo, J.; Williams, R. J. J. *Macromol. Chem. Phys.* **2004**, *205*, 676.
(46) Noshay, A.; Robeson, L. M. *J. Polym. Sci., Part A: Polym. Chem.* **1974**, *12*, 689.
(47) Clark, J. N.; Daly, J. H.; Garton, A. *J. Appl. Polym. Sci.* **1984**, *29*, 3381.
(48) Chen, J. L.; Chang, F.-C. *Macromolecules* **1999**, *32*, 5348.
(49) Ni, Y.; Zheng, S. *Polymer* **2005**, *46*, 5828.
(50) Meng, F.; Zheng, S.; Liu, T. *Polymer* **2006**, *47*, 7590.
(51) Tanaka, H.; Nishi, T. *Phys. Rev. A* **1989**, *39*, 783.
(52) Rasband, W. S. *ImageJ*; National Institutes of Health: Bethesda, MD, 2007. Please see http//rsb.info.nih.gov/ij/index.html, accessed July 2009.
(53) Sanja, Z. N.; Kupehela, L. *Polym. Eng. Sci.* **1976**, *28*, 1149.
(54) Ochi, M.; Okasaki, M.; Shimbo, M. *J. Polym. Sci., Part B: Polym. Phys.* **1982**, *20*, 89.
(55) Shibanov, Y. D.; Godovsky, Y. K. *Prog. Colloid Polym. Sci.* **1989**, *80*, 110.
(56) van Krevelen, D. W. *Properties of Polymers, Their Correlation with Chemical Structures; Their Numerical Estimation and Prediction from Additive Group Contributions*, 4th ed.; Elsevier: Amsterdam, 2009; p 215.
(57) Flory, P. J. *Principles of Polymer Chemistry*; Cornell University Press: Ithaca, NY, 1953;
(58) Stockmayer, W. H. *J. Chem. Phys.* **1943**, *11*, 45.
(59) Huang, M. J.; Williams, J. G. *Macromolecules* **1994**, *27*, 7423.
(60) Calado, V. M.A.; Advanni, S. G. In *Processing of Composites*; Davé, R. S.; Loos, A. C., Eds.; Hanser Publishers: Munich, Germany, 1999; p 41.
(61) Clarkw, N.; McLeish, T. C. B.; Jenkins, S. D. *Macromolecules* **1995**, *28*, 4650.